


## Article

# An Experimental Study on the Effect of Nanofluids on the Thermal Conductivity and Rheological Properties of a Coolant for Liquids

Le Sun <sup>1,\*</sup> , Jiafeng Geng <sup>2</sup>, Kaijun Dong <sup>1</sup> and Qin Sun <sup>1</sup>

<sup>1</sup> Guangzhou Institute of Energy Conversion, Chinese Academy of Sciences, Guangzhou 510640, China; dongkj@ms.giec.ac.cn (K.D.); sunqinsq@hotmail.com (Q.S.)

<sup>2</sup> School of Water and Environment, Chang'an University, Xi'an 710064, China; gengjf@chd.edu.cn

\* Correspondence: sunyuexuzhou@hotmail.com; Tel.: +86-020-38455713

**Abstract:** Thermal conductivity and viscosity are important properties for nanofluids as they significantly affect the flow and heat transfer process. To date, the rheological properties of water-based nanofluids have been well studied, while the results are scarce for non-aqueous nanofluids. In this study, the thermal conductivity and rheological properties of two different kinds of oxide nanofluids (CuO and Al<sub>2</sub>O<sub>3</sub>) in a typical commercial data center focusing on liquid coolants were systematically investigated at different mass fractions and temperatures. The results showed that the addition of nanoparticles can significantly improve the heat conduction capacity of mineral oil coolants. There is an average increase in thermal conductivity of up to 20–25%. The shear rate–shear stress and shear rate–viscosity curves all showed that mineral oil coolant-based oxide nanofluids behaved as Newtonian fluids and that nanoparticles did not cause the increment in viscosity. The effect of temperature on rheological properties was also studied, and the result showed that high temperatures resulted in low viscosity and shear stress. Finally, the effect of particle type was investigated, and it was found that no matter what kind of nanoparticles were added, their effects on the rheological behaviors were the same.



**Citation:** Sun, L.; Geng, J.; Dong, K.; Sun, Q. An Experimental Study on the Effect of Nanofluids on the Thermal Conductivity and Rheological Properties of a Coolant for Liquids. *Energies* **2024**, *17*, 1313.

<https://doi.org/10.3390/en17061313>

Academic Editors: Robert A. Varin and Geng Zhong

Received: 19 January 2024

Revised: 29 February 2024

Accepted: 7 March 2024

Published: 8 March 2024



**Copyright:** © 2024 by the authors. Licensee MDPI, Basel, Switzerland. This article is an open access article distributed under the terms and conditions of the Creative Commons Attribution (CC BY) license (<https://creativecommons.org/licenses/by/4.0/>).

**Keywords:** liquid cooling; nanofluids; heat conductivity; viscosity; rheology

## 1. Introduction

Nanofluids have attracted much attention in the past several years thanks to the small sizes and large specific surface areas of nanoparticles [1–9]. In general, nanofluids are defined as a new kind of heat transfer fluid with nanosized particles dispersing into conventional working fluids, such as water, methanol, ethanol, glycol and oil [10,11]. Various metallic or nonmetallic nanoparticles can be applied to form nanofluids, for example, Cu, CuO, Al<sub>2</sub>O<sub>3</sub>, SiO<sub>2</sub>, TiO<sub>2</sub>, Fe<sub>3</sub>O<sub>4</sub>, etc. [12–24]. Many researchers have found that compared to fluids without nanoparticles, nanofluids have many superior features, such as enhanced solar energy absorption, high heat transfer efficiency, an enhanced rate of oil and gas recovery and other properties related to spreading, wetting and antibacterial activity [25].

To date, most informed research studies regarding nanofluids have only focused on the behaviors during the thermal conduction, convective heat transfer and phase change heat transfer processes. Although very little attention has been paid to the rheological properties of nanofluids, especially for nanofluids applied in the data center cooling process, rheological properties play equally significant roles as thermal parameters in the engineering applications and parameters of nanofluids. For example, the viscosity of working fluids has a tight relation with pressure drop, which determines the power of the pump. Overall, from the point view of engineering applications, it is valuable to find ideal nanofluids that not only have high thermal conductivity, but also possess low viscosity.

The most widely used metal nanoparticle in the literature is Cu. Leong [18] investigated the heat transfer enhancement of ethylene glycol-based copper nanofluids in an automotive cooling system. The volume concentration of nanoparticles they used ranged from 0% to 2%, and they studied the heat transfer rate in different air and coolant conditions with different Reynolds numbers. They found that with the increase in nanoparticles, the heat transfer rate can increase by up to 3.8%. The increase in the Reynolds number also has an effect on the heat enhancement of Cu-ethylene glycol nanofluids. When the air's Reynolds number was increased from 4000 to 6000, the heat transfer rate showed a 45.2% enhancement. But when the Reynolds number of the coolant was increased from 5000 to 7000, the enhancement of the heat transfer rate was not obvious (only 0.4%).

Another commonly used metal nanoparticle is Ag. Behrangzade and Heyhat [26] compared the effect of using nano-silver–water nanofluid and pure water for energy efficiency enhancement at the same flow rate and same Reynolds number, respectively. By using 100 ppm of nano-silver dispersed water-based nanofluid, they obtained a 16.79% enhancement in the overall heat transfer coefficient, while the pressure drop value did not exhibit an obvious change.

Al<sub>2</sub>O<sub>3</sub> nanofluids are the most widely investigated type of nanofluids in the literature. Hassani et al. [27] used different volume fractions of Al<sub>2</sub>O<sub>3</sub> nanoparticles to synthesized nanofluids. Al<sub>2</sub>O<sub>3</sub> nanofluids were used as nanofluid coolants for an electronic heat sink. The results disclosed that Al<sub>2</sub>O<sub>3</sub> nanofluids with 0.5% and 1.0% volume fractions can enhance the performance index of the heat sink by averages of 14.7% and 28.3%.

Al<sub>2</sub>O<sub>3</sub>–water nanofluids were used by Nguyen [28] in an electronic liquid cooling system. Among the different volume concentrations of Al<sub>2</sub>O<sub>3</sub>–water nanofluids tested in their experiments, it was found that 6.8% of the Al<sub>2</sub>O<sub>3</sub> particle can enhance the heat transfer coefficient by 40% compared to pure water. And the particle size also has an effect on heat transfer. A 36 nm Al<sub>2</sub>O<sub>3</sub> particle is better at enhancing heat transfer coefficients than a 47 nm particle.

CuO is another commonly studied nanosized metal oxide material. Chein and Chuang [29] designed a series of experiments to investigate the effect of using a CuO–water nanofluid as a coolant. The CuO particle volume fraction ranges from 0.2% to 0.4% in nanofluids. The authors found that a CuO–water nanofluid can take away more heat than pure water in a microchannel heat sink at a low flow rate. But when the flow rate is high, the nanofluid has little effect on extra heat transfer and the heat transfer is mainly affected by the volume flow rate.

The performance of a CuO–water nanofluid in a heat sink was also studied by Sarafraz [30]. A CuO–water nanofluid, gallium liquid metal and water were used to transfer the heat of a CPU when it worked separately at three states (standby, normal and overload). Compared to the other two working fluids, a CuO–water nanofluid can provide higher thermal performance than water and lower pressure drop and pumping power than gallium liquid metal when the heat flux is not very high.

The heat transfer performance and rheological properties of a coolant are important for the practical application of liquid cooling in data centers. To date, the heat transfer and rheological properties of water-based nanofluids have been sufficiently investigated. However, both the thermal conductivity and viscosity of nanofluids based on data center coolants have rarely been studied. Thus, in the present work, we report on the synthesis of nanofluids based on a data center coolant containing CuO and Al<sub>2</sub>O<sub>3</sub> nanoparticles separately. We also measure and analyze their thermal conductivity and rheological behaviors, including shear stress and viscosity. Additionally, the effects of temperature, particle type and volume fraction are fully investigated and discussed. Our experimental work will be useful for the optimal design of various electronic components in cooling processes that use nanofluids as working fluids.

## 2. Materials and Methods

### 2.1. Materials and Preparation

Commercially available data center coolant (YT198, purchased from Amer Technology Co., Ltd., Dongguan, China) was used as base fluid. The basic parameters of the coolant are listed below (see Table 1). Various volume fractions of CuO (40 nm, Macklin Biochemical Cooperation, Shanghai, China) and Al<sub>2</sub>O<sub>3</sub> (80 nm, Sinopharm Chemical Reagent Cooperation, Shanghai, China) nanofluids, respectively, were formulated. And then the rheological properties of the nanofluids were investigated with a rotating rheometer (Haake Mar 60, Thermo Fisher Scientific Inc., Waltham, MA, USA) over a shear rate ranging from 0 s<sup>-1</sup> to 100 s<sup>-1</sup>.

**Table 1.** Typical properties of coolant (YT198) used for this study.

<b>Density (20 °C)</b>	<b>Pour Point</b>	<b>Flash Point</b>	<b>Acidity</b>	<b>Specific Heat (40 °C)</b>
804.3 kg/m <sup>3</sup>	−38 °C	198 °C	0.03 mgKOH/g	2.089 KJ/kg·K
<b>Breakdown Voltage</b>	<b>Relative Permittivity (90 °C)</b>	<b>Volume Resistivity (20 °C)</b>	<b>Surface Tension</b>	<b>Global Warming Potential</b>
62 KV	2.039	1.9 × 10 <sup>10</sup> Ω·cm	16 mN/m	0

Table 2 shows the typical properties of the nanoparticles employed for this study; the properties were measured with reliable accuracy by reagent manufacturers.

**Table 2.** Typical properties of nanoparticles employed for this study.

<b>Nanoparticle</b>	<b>Particle Size</b>	<b>Density (20 °C)</b>	<b>Melting Point</b>	<b>Boiling Point</b>
CuO	40 nm	6.315 g/cm <sup>3</sup>	1326 °C	1026 °C
Al <sub>2</sub> O <sub>3</sub>	80 nm	1.06 g/cm <sup>3</sup>	2000 °C	2977 °C

In order to disperse nanoparticles into the base fluid fully and uniformly, an ultrasonic homogenizer was applied in this experiment. The ultrasonic homogenizer (YT-JY99-IIDN, Shanghai Yetuo Technology Co., Ltd., Shanghai, China) has a max power of 1800 W, and the diameter of its ultrasonic horn is 22 mm. A picture of the ultrasonic homogenizer used in this work is shown in Figure 1. The main reasons for our choice of these kinds of nanoparticles are that they can be easily obtained in industry and their chemical properties are very stable but not harmful to human beings.



**Figure 1.** The ultrasonic homogenizer used in this work.

To start the experiment, the two kinds of nanoparticles with different volume fractions were added into the coolant using the following two-step method. The relationship between mass fraction and volume fraction is listed hereinafter (see Equation (1)):

$$\varphi = \frac{\omega \cdot \rho_{bf}}{\left(1 - \frac{\omega}{100}\right) \rho_p + \frac{\omega}{100} \rho_{bf}} \quad (1)$$

In this equation,  $\varphi$  and  $\omega$  stand for volume fraction and mass fraction, respectively, while  $\rho$  represents the density of the two different kinds of nanoparticles, and subscripts  $p$  and  $bf$  stand for particles and base fluid, respectively.

Firstly, the different kinds of nanoparticles were accurately weighed using an electronic balance and were then added in a methanol base fluid. The mass fractions investigated in our study are 0.01%, 0.05%, 0.1% and 0.15%, respectively. After that, the mixtures of the nanoparticles and base fluid were placed into an ultra-sonic homogenizer so that the nanoparticles could be fully and uniformly dispersed in the coolant. After 3 h of ultrasonic treatment, the methanol-based CuO and Al<sub>2</sub>O<sub>3</sub> nanofluids were ready for use. And then a certain volume of nanofluids (19 mL) was taken out as a sample, and the rheological investigation was conducted.

## 2.2. Thermal Conductivity and Rheological Investigation

Thermal conductivity was measured using HotDisk TPS2500S (Hotdisk AB, Co., Ltd., Gothenburg, Sweden). A photo of the thermal conductivity measure system is shown in Figure 2. More details about the instrument can be found in reference [31].



**Figure 2.** HotDisk TPS2500S, used to measure thermal conductivity.

A Haake Mars 60 rheometer (See Figure 3) was mainly used for the rheological measurement. The temperature was controlled by a refrigerated circulating bath connected with the rheometer. A schematic diagram of the apparatus is given in Figure 3. More details about this rheometer can be found in reference [32].



**Figure 3.** Haake Mars 60 rheometer used to study the rheological behavior.

The shear stress and viscosity of CuO-YT198 and Al<sub>2</sub>O<sub>3</sub>-YT198 at various volume fractions (0.01%, 0.05%, 0.1% and 0.15%) were measured through two programmed modes, respectively: shear rate sweep and temperature sweep. In shear rate sweep mode, the shear rates were increased from 0 s<sup>-1</sup> to 100 s<sup>-1</sup> at 25 °C; at the same time, the shear stress and viscosity were measured. For temperature sweep, the temperature rose from 25 to 70 °C at a heating rate of 1 °C/min. At the same time, shear stress and viscosity were measured, while the shear rate was fixed at 50 s<sup>-1</sup>.

## 2.3. Experimental Uncertainty

The thermal conductivity ( $k$ ) was calculated according to Fourier's Law [33] using Equation (2):

$$k = \frac{q \times s}{\Delta T} \quad (2)$$

where  $q$  is the measured heat flux ( $\text{W}/\text{m}^2$ ) on the face of the wall specimen,  $s$  is the thickness of the wall specimen (meters) and  $\Delta T$  is the temperature difference between the two wall specimens' faces ( $^{\circ}\text{C}$ ).

The sensors were calibrated, and the uncertainty of each of sensor was  $\pm 0.01$   $^{\circ}\text{C}$  (temperature sensor),  $\pm 0.1$   $\text{W}/\text{m}^2$  (heat flux sensor) and  $\pm 0.01$  mm (caliper for specimen thickness). The uncertainty of the final thermal conductivity result was associated with the propagation of uncertainty of indirect experimental measurements [34]. The calculated uncertainty propagation for thermal conductivity is  $\pm 0.00005$   $\text{W}/\text{m}\cdot\text{K}$ .

The error value of the rheological measurements depended on the rheological measurement device used and its settings. The whole set of the determined characteristics was defined by repeating experiments under identical initial conditions. Many factors can result in random errors, for example, uncontrolled vibrations during measurements [35]. To process the results, including the identification and elimination of gross errors, standard approaches [36] were used, including calculating the mathematical expectation (Equation (4)), variance of a random variable (Equation (5)), and standard deviation for each series (Equation (6)).

$$M_x = \frac{1}{n} \sum_{i=1}^n X_i \quad (3)$$

$$V = \frac{1}{n-1} \sum_{i=1}^n (X_i - M_x)^2 \quad (4)$$

$$\sigma = V^{1/2} \quad (5)$$

where  $M_x$  is the mathematical expectation;  $X_i$  is the measurement result;  $n$  is the number of measurements;  $V$  is the variance; and  $\sigma$  is the standard deviation. The calculated uncertainty propagation for the viscosity is  $\pm 0.017$   $\text{mPa}\cdot\text{s}$ .

### 3. Results and Discussion

#### 3.1. The Basic Properties of the Investigated Nanofluids

The particle size distribution and morphology of the particles not only affect the dispersion stability of the nanofluid, but also the heat transfer characteristics [37]. A large number of studies have shown that the optimization of the effective thermal conductivity is a function of particle size reduction. This effect is even more obvious when the fluid temperature and particle concentration increase.

When the particle size is less than 100 nm, the thermal conductivity decreases with the increase in particle size. Beyond this particle size, further increases in particle size do not have effects on the effectiveness of thermal conductivity. However, even for the same nanofluid, the rate of change of thermal conductivity with nanoparticle size distribution at the same particle concentration and fluid temperature has different conclusions in different studies.

Figure 4a,b exhibit SEM images of CuO and  $\text{Al}_2\text{O}_3$ , respectively. The shapes and morphologies of the employed nanoparticles in our experiments can be seen in this figure. In Figure 4, one can see that the average size of a CuO nanoparticle is 40 nm, which conforms to the declared diameter, while the average size of an  $\text{Al}_2\text{O}_3$  nanoparticle is 35 nm, which is much less than its declared diameter.

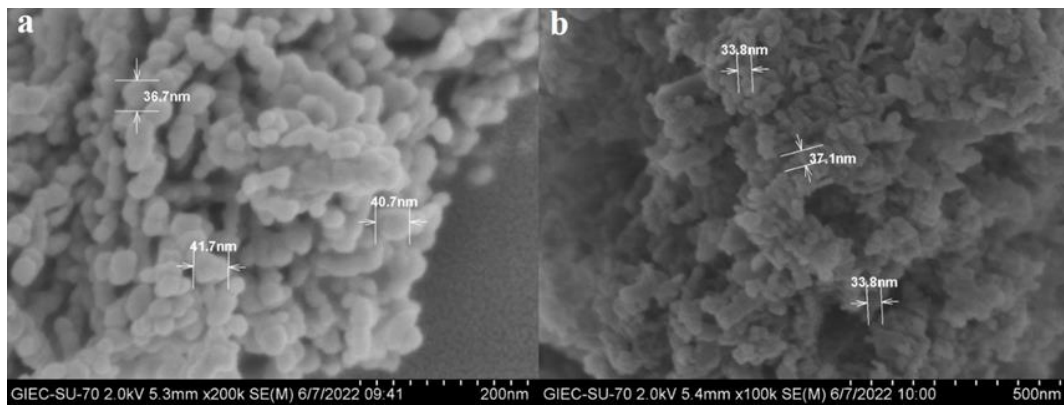


**Figure 4.** SEM images of (a) CuO and (b) Al<sub>2</sub>O<sub>3</sub> nanoparticles.

### 3.2. Thermal Conductivity Enhancement of Nanofluids

In the following study, the effects of adding different volume fractions of nanoparticles are discussed. Before measuring the thermal conductivity of the nanoparticle coolant system, the thermal conductivity was tested, and the result is shown in Figure 5. As we can see from Figure 5, the thermal conductivity of pure YT198 was 0.1390 and 0.1450 W/(m·K) at 25 °C and 55 °C, respectively. After the addition of CuO and Al<sub>2</sub>O<sub>3</sub> nanoparticles, the thermal conductivity increased obviously, regardless of the amount and kind of nanoparticles and the temperature.

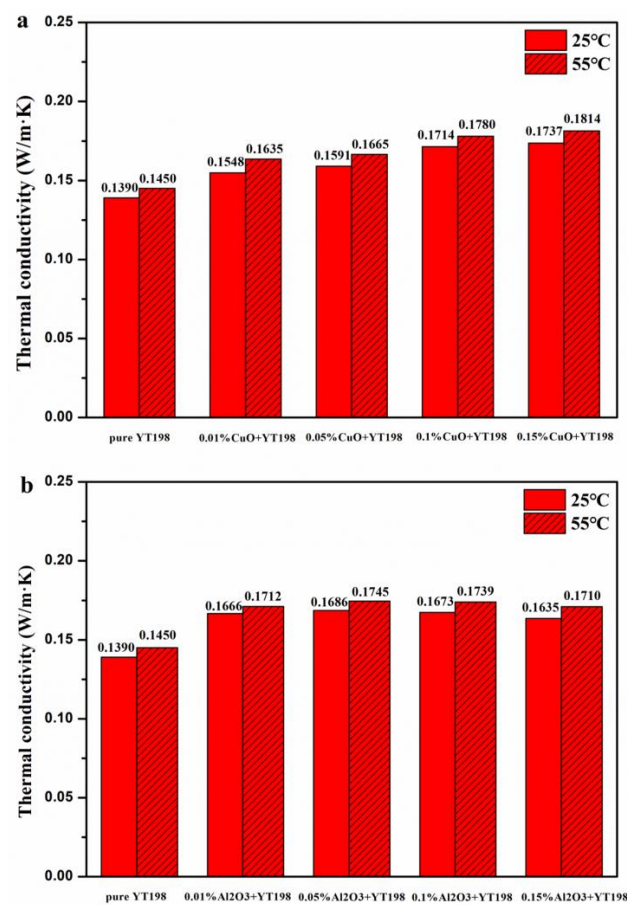


**Figure 5.** Thermal conductivity of pure coolant and coolant with different volume fractions: (a) CuO and (b) Al<sub>2</sub>O<sub>3</sub> nanoparticles.

In Figure 5a, one can see that with the increment in the CuO nanoparticle's volume fraction, the thermal conductivity also increased with monotony; when the volume concen-

tration of CuO nanoparticles was 0.15%, the thermal conductivity reached 0.1737 W/(m·K) at 25 °C and 0.1814 W/(m·K) at 55 °C. Compared with pure YT198, these growths in thermal conductivity represent growths of 20% and 25%, respectively.

Temperature variations affect the dispersion of nanoparticles in base fluids. High temperatures can result in more intense Brownian motion. Thus, the aggregation and sedimentation of nanoparticles can be hindered.

Similar laboratory findings can also be seen in Figure 5b; the addition of very few Al<sub>2</sub>O<sub>3</sub> nanoparticles (0.01%) can cause a great enhancement in thermal conductivity from 0.1390 and 0.1450 W/(m·K) to 0.1666 and 0.1712 W/(m·K) at 25 °C and 55 °C, respectively, and the increasing percentages can be as large as 20% and 18%. But the growth trend is not synonymous with the volume of nanoparticles. The largest enhancement in thermal conductivity occurred when the volume fraction of Al<sub>2</sub>O<sub>3</sub> + YT198 nanofluids was 0.05%; the increasing percentage reached 20% and 21% compared with the pure coolant. When comparing Figure 5a,b, it can be seen that the CuO nanoparticles had a slightly more significant improvement in thermal conductivity than the Al<sub>2</sub>O<sub>3</sub> nanoparticles overall.

A possible explanation for the better thermal conductivity enhancement of the CuO nanoparticle in comparison to that of the Al<sub>2</sub>O<sub>3</sub> nanoparticle is that CuO nanoparticles have greater conductivity [38]. Furthermore, as the number of nanoparticles increases, there may be more rapid interactions between the nanoparticles, and the Brownian motion of the nanoparticles may increase accordingly.

Durga Bhavani et al. observed that Al<sub>2</sub>O<sub>3</sub> nanofluids had high compressibility at a high concentration [39]. When the concentration of Al<sub>2</sub>O<sub>3</sub> nanofluids increased, the bulk modulus also increased, and the adiabatic compressibility decreased, which led to a strong cohesive interaction force among the molecules and atoms. Al<sub>2</sub>O<sub>3</sub> particles tend to move less freely, and the Brownian motion of these nanoparticles also decreases. This may explain the decrease in thermal conductivity when the concentration of Al<sub>2</sub>O<sub>3</sub> nanofluids surpassed 0.1%.

Surface modifications of nanoparticles contribute to the enhanced properties of nanofluids through the anti-aggregation effect produced by surface-modified nanoparticles. As studied by Linyang Dan. et al. [40], due to the Coulombic energy from the heteroatoms of SiO<sub>2</sub> nanoparticles, nanoparticles lacking alkyl chains can form aggregates and show a strong tendency to approach each other. By grafting alkyl chains on the surfaces of SiO<sub>2</sub> nanoparticles, Coulombic interactions can be shielded effectively, and the van der Waals interaction with natural esters can increase. Thus, the aggregation tendency of nanoparticles can be reduced. Furthermore, surface modification can reduce the diffusion ability of nanoparticles under the steric hindrance effect, thereby inhibiting the collision and aggregation of nanoparticles.

The pH mainly affects nanofluids in the following two aspects: the stability of nanofluids and the surface tension of nanofluids [41]. By adjusting the pH, the surface tension of a nanofluid can be changed. A pH value that is too high or too low can lead to corrosion and rusting [42].

Surfactants can increase the stability of nanofluids. The addition of surfactants does not have a great effect on the thermal conductivity, but it can increase the viscosity of the nanofluid.

The thermal conductivity of the base fluid has a great influence on the thermal conductivity of the nanofluid. The thermal conductivity of water-based nanofluids is generally higher than that of other nanofluids. The thermal conductivity of synthetic oil-based nanofluids is greater than that of water-based nanofluids mainly because synthetic oil-based nanofluids are more stable.

### 3.3. Rheological Properties of Various Nanofluids at Different Shear Rates

As typical experimental results, Figure 6 shows the shear stress vs. shear rate curve of a pure coolant and various nanofluids with different volume fractions at room temperature. In Figure 6, we can see that regardless of whether nanoparticles were added or not, pure

YT198 and nanofluids all exhibited properties of Newtonian fluids. The shear stress of pure YT198 and nanofluids showed linear monotonic growth as the shear rate increased. For example, in the case of CuO nanofluids, there is a small increase in the shear stress after adding CuO nanoparticles compared to pure coolant. But there is little difference between various volume fractions of CuO nanofluids. This trend is consistent with the findings of our previous works [43,44]. In our previous work [43], we found that with the mass fractions of CuO, Cu<sub>2</sub>O and TiO<sub>2</sub> being increased from 0.01% to 0.15%, the viscosity showed almost no obvious change.

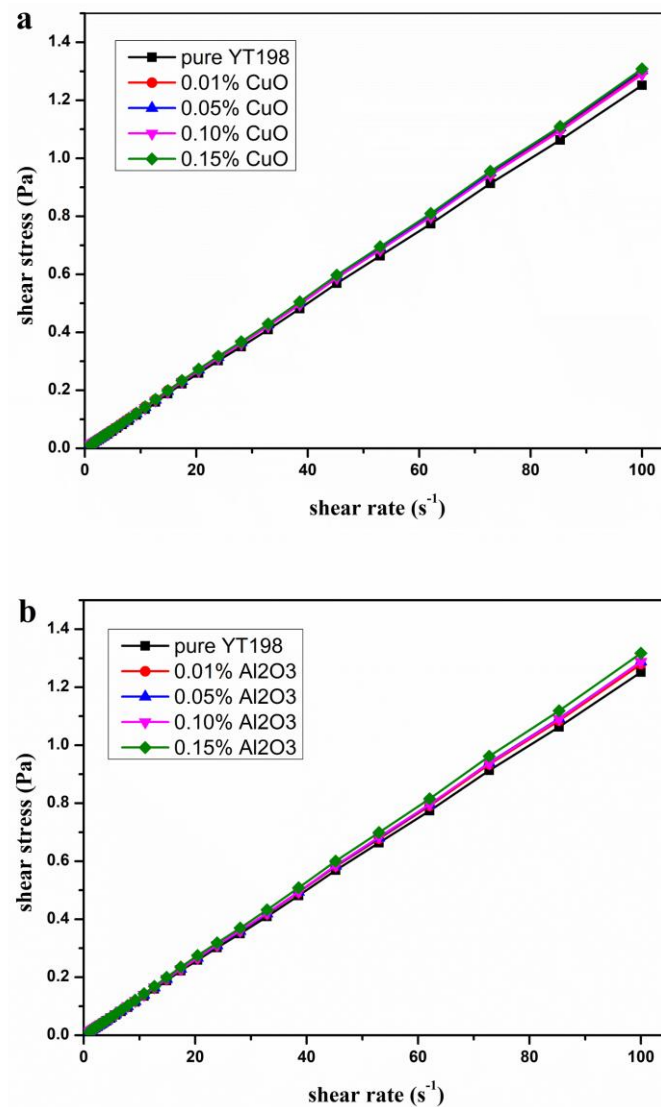


**Figure 6.** Shear stress vs. shear rate for various nanofluids with different volume fractions of (a) CuO and (b) Al<sub>2</sub>O<sub>3</sub> nanoparticles at 25 °C.

The Al<sub>2</sub>O<sub>3</sub> nanofluids also showed similar trends, and 0.15% Al<sub>2</sub>O<sub>3</sub> nanofluids showed the highest shear stress. One explanation for this phenomenon may be the low levels of nanoparticle addition. The shear stress of the base fluids cannot be changed if the concentration of nanoparticles is too low. Another important factor influencing the shear stress–shear rate curve is temperature. When the temperature is low (25 °C, as is shown in Figure 6), the interactions between the molecules and the Brownian motion are not strong. Thus, the shear stress does not show an obvious change despite the concentration being increased.

The comparison of viscosity between pure YT198 and nanofluids is also shown in Figure 7. In Figure 7, one can see that the viscosity increased with the increasing shear



rate before the shear rate reached  $20 \text{ s}^{-1}$ , and then, after a slight decline, the viscosity of both pure YT198 and nanofluids tended to achieve stable values. For the CuO nanofluids (Figure 7a), the descending order of viscosity values at the same shear rate is  $0.15\% > 0.05\% > 0.01\% > 0.10\% > \text{pure YT198}$ ; the maximum increase in viscosity occurred between pure YT198 and 0.15% CuO at  $20 \text{ s}^{-1}$  (5.34%). And the various numbers of nanoparticles added did not show obvious differences.

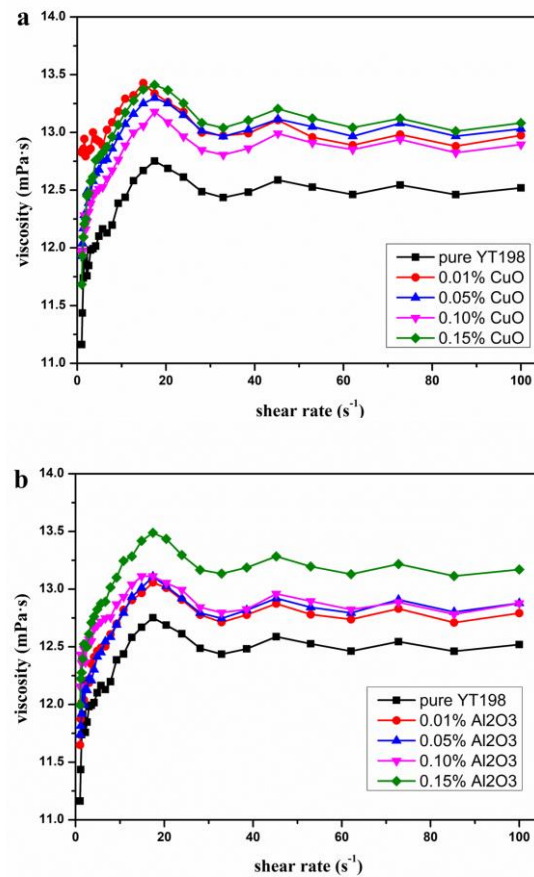


**Figure 7.** Viscosity vs. shear rate for various nanofluids with different volume fractions of (a) CuO and (b)  $\text{Al}_2\text{O}_3$  nanoparticles at  $25^\circ\text{C}$ .

As shown in Figure 7b, the addition of  $\text{Al}_2\text{O}_3$  nanoparticles also caused the viscosity to increase. The greater the concentration of nanoparticles added, the more obvious the increase in viscosity as follows:  $0.15\% > 0.01\% = 0.05\% = 0.10\% > \text{pure YT198}$ .

### 3.4. Effects of Temperature on Rheological Properties of Nanofluids

In this section, the different volume fractions (0.01%, 0.05%, 0.1% and 0.15%) of nanoparticles will be discussed in order to study the effect of temperature on their rheological properties. It was first found, as shown in Figure 8, that with the increment in temperature, the shear stress decreased exponentially. And one can see that various volume fractions of nanoparticles have little effect on the shear stress. This result is different from that obtained by Amir Yousuf Bhat and Adnan Qayoum [45]. They measured the viscosity of CuO nanofluids and reported a maximum increase of 0.5% in viscosity. The main reason why the results of our experiments differ from those in the literature is that the volume concentrations they used were between 1% and 4%, which are much larger than those used in this work.

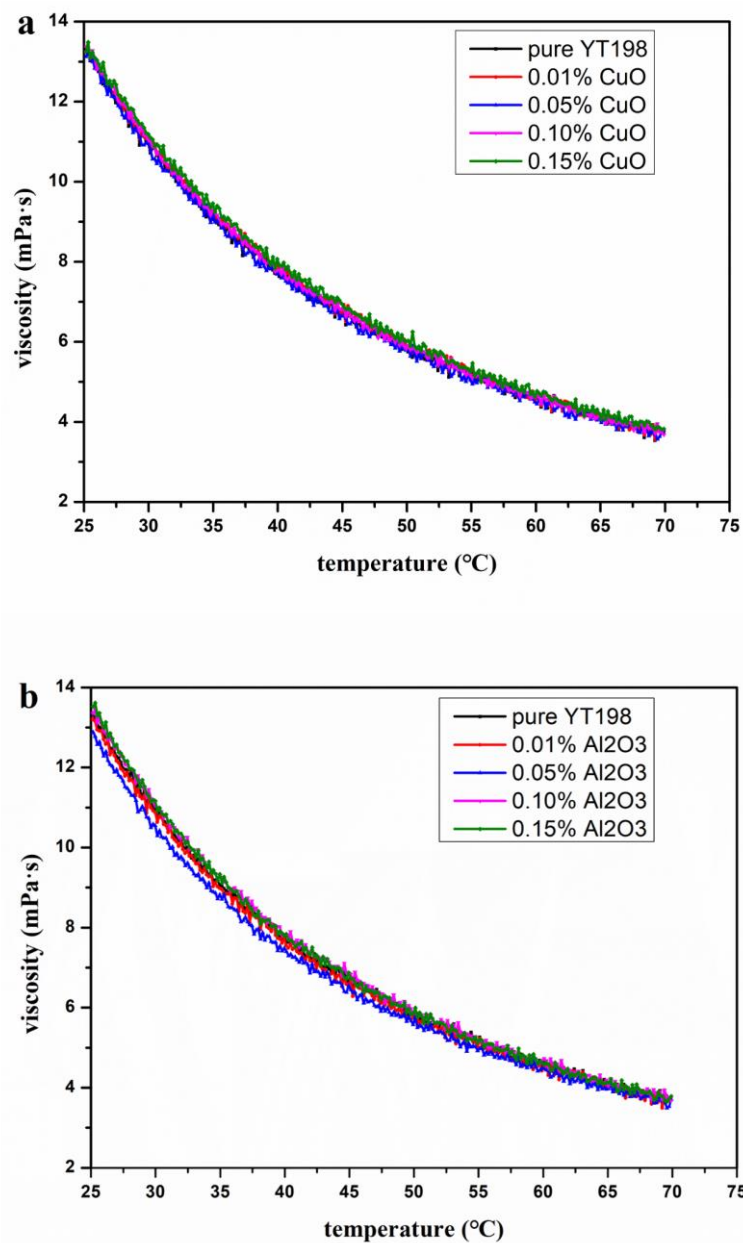


**Figure 8.** Effect of temperature on shear stress of pure YT198 and nanofluids at shear rate of  $50 \text{ s}^{-1}$ . (a) CuO; (b) Al<sub>2</sub>O<sub>3</sub>.

Additionally, the viscosity of CuO-YT198 and Al<sub>2</sub>O<sub>3</sub>-YT198 at different volume concentrations can be analyzed in Figure 9. As shown in Figure 9a,b, the results are consistent with the trend found in the study by Madhusree Kole and T.K. Dey [46]. Their results show that the viscosity of a nanofluid increases with an increasing nanoparticle concentration and decreases with an increase in temperature. The viscosity of these nanofluids decreased sharply with the increase in temperature, and the decreasing trend was also non-linear, which also illustrated that these mineral oil-based nanofluids are fluids whose rheological properties are strongly temperature-dependent. By comparing Figures 8 and 9 with the work of Amir Yousuf Bhat and Adnan Qayoum, we can see that a small number of nanoparticles can enhance heat transfer without causing a significant increase in viscosity.

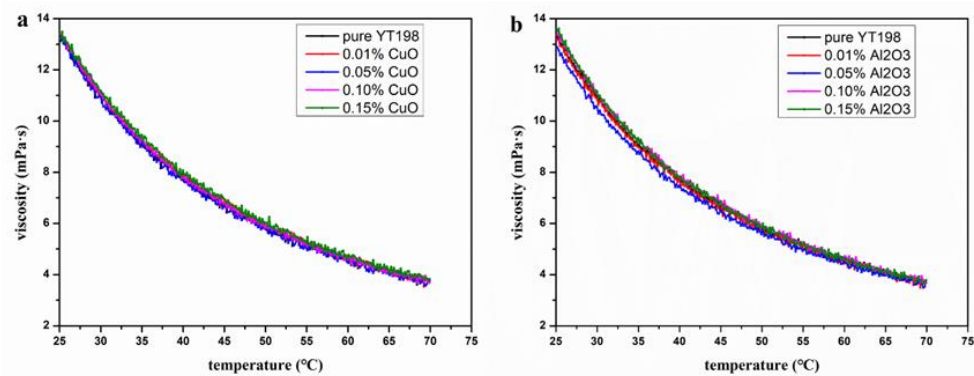


**Figure 9.** Effect of temperature on viscosity of pure YT198 and nanofluids at shear rate of  $50 \text{ s}^{-1}$ . (a) CuO; (b)  $\text{Al}_2\text{O}_3$ .

The stability of nanofluids is affected by temperature. Temperature variations affect the dispersion of nanoparticles in base fluids. High temperatures can result in more intense Brownian motion. Thus, the aggregation and sedimentation of nanoparticles can be hindered [47].

The nanofluid does not contain nitrogen, sulfur or aromatic hydrocarbons. So, over the course of long-term use, the color of the coolant will not turn yellow due to oxidation, which is a very common occurrence in other traditional cooling media. It will not form paint film and oil scale on electronic components. All of these characteristics ensure that the cooling medium has a long service life of more than 6 years and greatly decrease the cost of the cooling medium.

The cooling medium is made of extremely stable synthetic materials. It has a very low acid value and does not contain mineral oil or aromatic hydrocarbons. Long-term experiments have proven that nanofluids will not produce hardening, cracking, deformation, discoloration, corrosion, adhesion or other phenomena. They are harmless to the common plastics, resins, non-ferrous metals, plating and other components of the server circuit board, hard disk, central processing unit, etc. Using nanoparticles can ensure the stable performance of the parts and long-term trouble-free operation.

### 3.5. Derivation of Empirical Correlation

In this subsection, a mathematical model used to predict thermal conductivity and four famous models used to predict viscosity were used to fit and compare our experimental values of viscosity.

The Maxwell model [48] was suggested to predict the thermal conductivity of a nanofluid, and it is shown in the following Equation (6):

$$\frac{k_{nf}}{k_{bf}} = \frac{2k_{bf} + k_{np} + 2\varphi(k_{np} - k_{bf})}{2k_{bf} + k_{np} - \varphi(k_{np} - k_{bf})} \quad (6)$$

The suggested model is best suited for a nanofluid with nanoparticles with spherical shapes and lower volume fractions; a comparison of the theoretical predictions with the experimental results is shown in Figure 10.

As can be seen in Figure 10a, the Maxwell model was fixed well with the experimental results of thermal conductivity. The error between the experimental value and the predicted value of the model for the thermal conductivity of CuO nanofluids is no more than 6.1%. At concentrations of 0.01% and 0.05%, the predicted values of the model were greater than those measured in the experiments. At concentrations of 0.1% and 0.15%, the model predicted values were smaller than those from the experimental measurements. When comparing Figure 10a,b, it can be seen that the model agrees better with  $\text{Al}_2\text{O}_3$ .

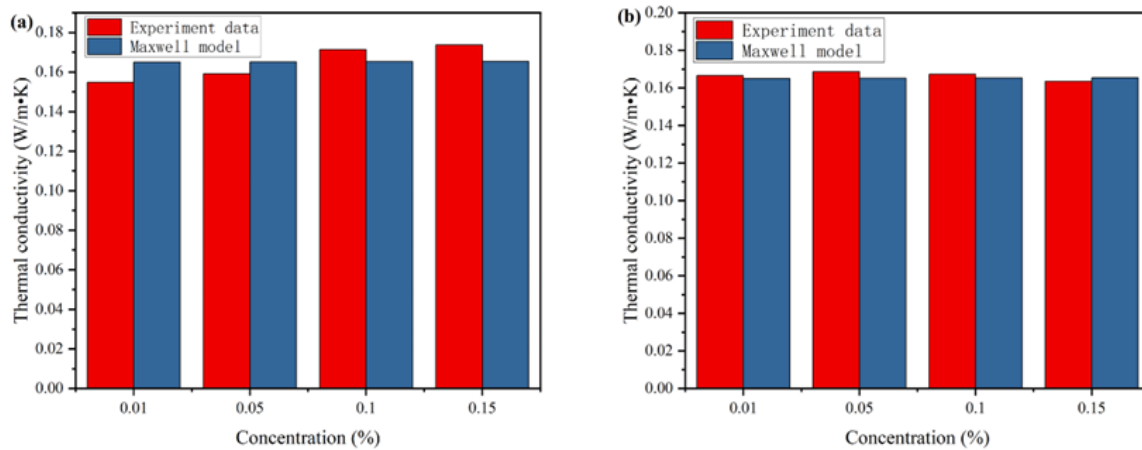


**Figure 10.** Comparison of theoretical predictions with experimental results of thermal conductivity at 25 °C for (a) CuO + YT198 and (b) 0.01% Al<sub>2</sub>O<sub>3</sub> + YT198.

The four famous rheological models we used to fit and compare with our experimental values were Einstein’s equation [49], Brinkman’s equation [50], Batchelor’s equation [51] and Wang et al.’s equation [52]. By using these four models, we could derive empirical correlations and then obtain quantitatively valuable insights into the YT198 coolant-based metal oxide nanofluid system. The equations of the four models are listed and briefly discussed in the following sections.

As the first theoretical model created to calculate the viscosity of mixtures and composites, the Einstein model has been widely proven to be valid in the case of mixtures with a volume fraction ( $\varphi$ ) of less than 0.02. The key assumption of the Einstein model is that the mixtures were simplified as linear viscous fluids and spherical particles. The equation for this model is as follows:

$$\mu_{nf} = \mu_{bf}(1 + 2.5\varphi) \quad (7)$$

Currently, the Brinkman-modified Einstein’s equation can be used for suspensions with volume fractions of up to 4%.

$$\mu_{nf} = \mu_{bf}(1 - \varphi)^{-2.5} \quad (8)$$

As a further modification, the existence of the Brownian motion effect was considered in the model proposed by Batchelor.

$$\mu_{nf} = \mu_{bf}(1 + 2.5\varphi + 6.5\varphi^2) \quad (9)$$

In 1999, Wang et al. [52] proposed another novel model to forecast the viscosity of nanofluids.

$$\mu_{nf} = \mu_{bf}(1 + 7.3\varphi + 123\varphi^2) \quad (10)$$

For all of the above equations,  $\mu$  represents the viscosity, and the subscripts  $nf$  and  $bf$  represent nanofluids and base fluids, respectively.  $\varphi$  represents the volume fraction of nanoparticles.

A comparison of the theoretical predictions with the experimental results at 20 °C is shown in Figure 11.

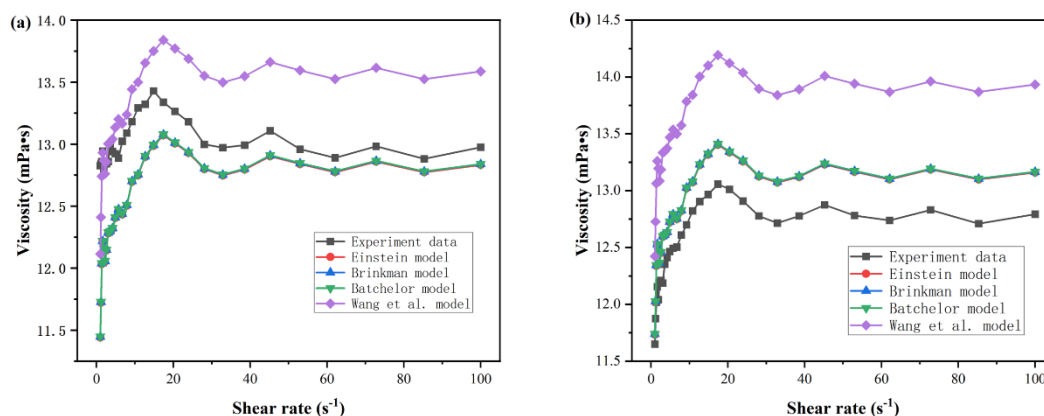


**Figure 11.** A comparison of the theoretical predictions with the experimental results at 20 °C for (a) 0.01% CuO + YT198 and (b) 0.01% Al<sub>2</sub>O<sub>3</sub> + YT198.

As shown in Figure 11, the predictions of the Brinkman model and the Batchelor model almost exactly coincide, mainly because the volume fraction of the nanofluid is too small. For CuO, the experimental prediction is made between the Wang model and the Brinkman model. As can be seen in (b), for Al<sub>2</sub>O<sub>3</sub>, all model predictions are higher than the experimental values. The biggest difference between the predicted value of the model and the experimental value is 20 s<sup>-1</sup>, and the errors are about 3.8% and 8.5%. Overall, the predicted and experimental values of the model are in good agreement. One possible reason for the model and experimental errors is that nanoparticles are not usually spherical.

#### 4. Conclusions

The thermal conductivity and rheological properties of two different kinds of oxide nanofluids (CuO and Al<sub>2</sub>O<sub>3</sub>) in YT198, a typical mineral oil coolant used for data center liquid cooling, were measured at different volume fractions and temperatures. The thermal conductivity measurement results showed that even adding a small number of nanoparticles can significantly improve the heat conduction capacity of mineral oil coolants. The average increase in thermal conductivity is 20–25%. The temperature of nanoparticles also has an effect on the rheological properties of methanol-based nanofluids. The higher the temperature, the lower the viscosity and shear stress. However, it was found that the type of nanoparticles has little effect on the rheological properties. The difference in the effect of adding copper oxide and aluminum oxide on the viscosity is not very obvious.

More experimental research studies are needed to obtain the best types of nanoparticle additives which have the best rheological parameters and the best thermal conductivity enhancement effects. A good rheological parameter can guarantee minimum flow energy consumption, and high thermal conductivity provides optimum heat transfer. Additionally, more characteristics such as the sizes, shapes and types of nanoparticles should be taken into consideration because they are essential to establish more numerical models for further studies of heat transfer and rheology.

Based on the outcomes of this study, several suggestions for future research are listed below:

1. There are several parameters that have influences on the effect of a nanofluid coolant, including but not limited to particle size and size distribution, particle shape and morphology, the concentration of nanoparticles and temperature. These factors must be comprehensively and adequately studied in future works.
2. The stability of nanofluids is critical for their use in practical applications. Thus, more investigations about the surface modifications of nanoparticles and the use of surfactants should be conducted in order to determine an appropriate surfactant with remarkable stability, moderate viscosity and thermal conductivity.

3. The long-term effects of using these nanofluids in cooling systems, such as corrosion or clogging, deserve more attention. A life cycle analysis (LCA) of cooling systems using nanofluids may be necessary to evaluate whether a nanofluid is suitable for long-term use.
4. There are various models that can predict the thermal conductivity and viscosity of nanofluids separately. In future works, more mechanisms such as Brownian diffusion, particle aggregation, thermomigration and nanolayer formation can be taken into consideration. Therefore, models that will be developed in the future can be more accurate.

**Author Contributions:** Conceptualization, L.S. and J.G.; methodology, L.S.; validation, L.S.; formal analysis, L.S.; investigation, L.S. and J.G.; resources, Q.S.; data curation, L.S.; writing—original draft preparation, L.S.; writing—review and editing, L.S.; visualization, L.S.; supervision, K.D.; project administration, K.D.; funding acquisition, K.D. and Q.S. All authors have read and agreed to the published version of the manuscript.

**Funding:** This research was funded by the Shenzhen Science and Technology Program, grant number KCXST20221021111216038, and Guangzhou Development Zone International Science and Technology Cooperation Project Funding, grant number 2021GH07.

**Data Availability Statement:** Data are contained within the article.

**Conflicts of Interest:** The authors declare no conflicts of interest.

## References

1. Patra, A.K.; Nayak, M.K.; Misra, A. Viscosity of nanofluids—A review. *Int. J. Thermofluid Sci. Technol.* **2020**, *7*, 070202. [[CrossRef](#)]
2. Nabil, M.F.; Azmi, W.H.; Hamid, K.A.; Mamat, R.; Hagos, F.Y. An experimental study on the thermal conductivity and dynamic viscosity of TiO<sub>2</sub>-SiO<sub>2</sub> nanofluids in water: Ethylene glycol mixture. *Int. Commun. Heat Mass Transf.* **2017**, *86*, 181–189. [[CrossRef](#)]
3. Khodadadi, H.; Toghraie, D.; Karimipour, A. Effects of nanoparticles to present a statistical model for the viscosity of MgO-Water nanofluid. *Powder Technol.* **2019**, *342*, 166–180. [[CrossRef](#)]
4. Saxena, G.; Raj, J. A critical review on applications of nano-fluid as coolant. *Int. J. Eng. Manag. Res.* **2017**, *7*, 304–311.
5. Saravanakumar, P.T.; Surya, M.; Vijay, D.; Santhoshkumar, G. Improving performance in engine cooling system using nano fluids. *Int. Res. J. Eng. Technol.* **2017**, *4*, 1495–1499.
6. Junior, L.C.C.; Nogueira, E. Influence of the coolant flow containing silver nanoparticles (Ag) from an aqueous solution based on ethylene glycol (EG50%) on the thermal-hydraulic performance of an automotive radiator. *World J. Nano Sci. Eng.* **2020**, *10*, 14. [[CrossRef](#)]
7. Sandhya, M.; Ramasamy, D.; Sudhakar, K.; Kadirgama, K.; Harun, W.S.W. Hybrid nano-coolants in automotive heat transfer—an updated report. *Maejo Int. J. Energy Environ. Commun.* **2023**, *2*, 43–57. [[CrossRef](#)]
8. Erkan, A.; Tüccar, G.; Tosun, E.; Özgür, T. Comparison of effects of nanofluid utilization (Al<sub>2</sub>O<sub>3</sub>, SiO<sub>2</sub>, TiO<sub>2</sub>) with reference water in automotive radiators on exergetic properties of diesel engines. *SN Appl. Sci.* **2021**, *3*, 365. [[CrossRef](#)]
9. Sundari, K.G.; Asirvatham, L.G.; Ninolin, E.; Surekha, B. Feasibility of Glycerin/Al<sub>2</sub>O<sub>3</sub> nanofluid for automotive cooling applications. *J. Therm. Eng.* **2020**, *6*, 619–632. [[CrossRef](#)]
10. Halelfadl, S.; Mare, T.; Estelle, P. Efficiency of carbon nanotubes water based nanofluids as coolants. *Exp. Therm. Fluid Sci.* **2014**, *53*, 104–110. [[CrossRef](#)]
11. Suganthi, K.S.; Rajan, K.S. Improved transient heat transfer performance of ZnO propylene glycol nanofluids for energy management. *Energy Convers Manag.* **2015**, *96*, 115–123. [[CrossRef](#)]
12. Asadi, A.; Pourfattah, F. Heat transfer performance of two oil-based nanofluids containing ZnO and MgO nanoparticles: A comparative experimental investigation. *Powder Technol.* **2019**, *343*, 296–308. [[CrossRef](#)]
13. Guo, W.; Li, G.; Zheng, Y.; Dong, C. Measurement of the thermal conductivity of SiO<sub>2</sub> nanofluids with an optimized transient hot wire method. *Thermochim. Acta* **2018**, *661*, 84–97. [[CrossRef](#)]
14. Abdolbaqi, M.K.; Sidik, N.A.C.; Rahim, M.F.A.; Mamat, R.; Azmi, W.H. Experimental investigation and development of new correlation for thermal conductivity and viscosity of BioGlycol/water based SiO<sub>2</sub> nanofluids. *Int. Commun. Heat Mass Transf.* **2016**, *77*, 54–63. [[CrossRef](#)]
15. Krishnakumar, T.S.; Sheeba, A.; Mahesh, V.; Jose, P.M. Heat transfer studies on ethylene glycol/water nanofluid containing TiO<sub>2</sub> nanoparticles. *Int. J. Refrig.* **2019**, *102*, 55–61. [[CrossRef](#)]
16. Perez-Tavernier, J.; Vallejo, J.P.; Cabaleiro, D.; Fernandez-Seara, J.; Lugo, L. Heat transfer performance of a nano-enhanced propylene glycol: Water mixture. *Int. J. Therm. Sci.* **2019**, *139*, 413–423. [[CrossRef](#)]
17. Yashawantha, K.M.; Vinod, A.V. ANN modelling and experimental investigation on effective thermal conductivity of ethylene glycol: Water nanofluids. *J. Therm. Anal. Calorim.* **2020**, *145*, 609–630. [[CrossRef](#)]

18. Leong, K.Y.; Saidur, R.; Kazi, S.N.; Mamun, A.H. Performance investigation of an automotive car radiator operated with nanofluid-based coolants (nanofluid as a coolant in a radiator). *Appl. Therm. Eng.* **2010**, *30*, 2685–2692. [[CrossRef](#)]
19. Subhedhar, D.G.; Ramani, B.M.; Gupta, A. Experimental investigation of heat transfer potential of Al<sub>2</sub>O<sub>3</sub>/Water-Mono Ethylene Glycol nanofluids as a car radiator coolant. *Case Stud. Therm. Eng.* **2018**, *11*, 26–34. [[CrossRef](#)]
20. Mhamed, B.; Sidik, N.A.; Akhbar, M.F.A.; Mamat, R.; Najafi, G. Experimental study on thermal performance of MWCNT nanocoolant in Perodua Kelisa 1000cc radiator system. *Int. Commun. Heat Mass Transf.* **2016**, *76*, 156–161. [[CrossRef](#)]
21. Goudarzi, K.; Jamali, H. Heat transfer enhancement of Al<sub>2</sub>O<sub>3</sub>-EG nanofluid in a car radiator with wire coil inserts. *Appl. Therm. Eng.* **2017**, *118*, 510–517. [[CrossRef](#)]
22. Kumar, A.; Hassan, M.A.; Chand, P. Heat transport in nanofluid coolant car radiator with louvered fins. *Powder Technol.* **2020**, *376*, 631–642. [[CrossRef](#)]
23. Said, Z.; El Haj Assad, M.; Hachicha, A.A.; Bellos, E.; Abdelkareem, M.A.; Alazaizeh, D.Z. Enhancing the performance of automotive radiators using nanofluids. *Renew Sustain. Energy Rev.* **2019**, *112*, 183–194. [[CrossRef](#)]
24. Tijani, A.S.; Sudirman, A.S. Thermo-physical properties and heat transfer characteristics of water/anti-freezing and Al<sub>2</sub>O<sub>3</sub>/CuO based nanofluid as a coolant for car radiator. *Int. J. Heat Mass Transf.* **2018**, *118*, 48–57. [[CrossRef](#)]
25. Muruganandam, M.; Mukesh Kumar, P.C. Experimental analysis on internal combustion engine using MWCNT/water nanofluid as a coolant. *Mater. Today Proc.* **2020**, *21*, 248–252. [[CrossRef](#)]
26. Behrangzade, A.; Heyhat, M.M. The effect of using nano-silver dispersed water based nanofluid as a passive method for energy efficiency enhancement in a plate heat exchanger. *Appl. Therm. Eng.* **2016**, *102*, 311–317. [[CrossRef](#)]
27. Hassani, S.M.; Khoshvaght, A.M.; Mazloumi, S.H. Influence of chevron fin interruption on thermo-fluidic transport characteristics of nanofluid-cooled electronic heat sink. *Chem. Eng. Sci.* **2018**, *191*, 436–447. [[CrossRef](#)]
28. Nguyen, C.T.; Roy, G.; Gauthier, C.; Galanis, N. Heat transfer enhancement using Al<sub>2</sub>O<sub>3</sub>-water nanofluid for an electronic liquid cooling system. *Appl. Therm. Eng.* **2007**, *27*, 1501–1506. [[CrossRef](#)]
29. Chein, R.; Chuang, J. Experimental microchannel heat sink performance studies using nanofluids. *Int. J. Therm. Sci.* **2007**, *46*, 157–166. [[CrossRef](#)]
30. Sarafraz, M.M.; Arya, A.; Hormozi, F.; Nikkhah, V. On the convective thermal performance of a CPU cooler working with liquid gallium and CuO/water nanofluid: A comparative study. *Appl. Therm. Eng.* **2017**, *112*, 1373–1381. [[CrossRef](#)]
31. Sun, S.; Jin, X.; Liu, C.; Meng, Q.; Zhang, Y. Study on in-situ measurement method of THF hydrate thermal conductivity. *Int. J. Heat Mass Transf.* **2018**, *127*, 88–96. [[CrossRef](#)]
32. Gu, C.; Lv, Y.; Fan, X.; Zhao, C.; Dai, C.; Zhao, G. Study on rheology and microstructure of phenolic resin cross-linked nonionic polyacrylamide (NPAM) gel for profile control and water shutoff treatments. *J. Pet. Sci. Eng.* **2018**, *169*, 546–552. [[CrossRef](#)]
33. Amaral, C.; Pinto, S.; Silva, T. Development of polyurethane foam incorporating phase change material for thermal energy storage. *J. Energy Storage* **2020**, *28*, 101177. [[CrossRef](#)]
34. Alex, R.; Alexander, M.T.; Gabriel, F.; Gaurav, S.; Laurent, P. Thermal conductivity of cementitious composites containing microencapsulated phase change materials. *Int. J. Heat Mass Transf.* **2017**, *104*, 71–82.
35. Maxim, P.; Daniil, R.; Pavel, S. Stability and rheology of carbon-containing composite liquid fuels under subambient temperatures. *Energy* **2023**, *278*, 127912.
36. Theodorsson, E. Uncertainty in measurement and total error: Tools for coping with diagnostic uncertainty. *Clin. Lab. Med.* **2017**, *37*, 15–34. [[CrossRef](#)] [[PubMed](#)]
37. Tehmina, A.; Man-Hoe, K. Influence of particle size on the effective thermal conductivity of nanofluids: A critical review. *Appl. Energy* **2020**, *264*, 114684.
38. Nishant, K.; Shiriram, S. Experimental study of thermal conductivity and convective heat transfer enhancement using CuO and TiO<sub>2</sub> nanoparticles. *Int. Commun. Heat Mass* **2016**, *76*, 98–107.
39. Durga, B.J.; Tami, S.G.; Subashini, G.; Saravanan, P.; Muthumareeswaran, M.; Abdullah, N.A.; Nirmala, G.A. Ultrasonic Interferometry and Physiothermal properties of Al<sub>2</sub>O<sub>3</sub>/CuO nanofluids. *Case Stud. Therm. Eng.* **2024**, *55*, 104120.
40. Dan, L.; Zhang, K.; Wang, Q.; Liu, N. Surface modification boosts dispersion stability of nanoparticles in dielectric fluids. *J. Ind. Eng. Chem.* **2024**, *132*, 518–528. [[CrossRef](#)]
41. Younes, H.; Mao, M.; Murshed, S.S.; Lou, D.; Hong, H.; Peterson, G.P. Peterson. Nanofluids: Key parameters to enhance thermal conductivity and its applications. *Appl. Therm. Eng.* **2022**, *10*, 118202. [[CrossRef](#)]
42. Yilmaz, D.A.; Gürü, M. Nanofluids: Preparation, stability, properties, and thermal performance in terms of thermo-hydraulic, thermodynamics and thermo-economic analysis. *J. Therm. Anal. Calorim.* **2022**, *147*, 7631–7664. [[CrossRef](#)]
43. Sun, L.; Zhang, Y.; Gao, W.; Li, X.; Jing, D. Rheology of methanol-based metal oxide nanofluids: The effect of temperature and particle type and mass fraction. *Interfacial Phenom. Heat Transf.* **2020**, *8*, 165–181. [[CrossRef](#)]
44. Sun, L.; Zhao, Q.; Zhang, Y.; Gao, W.; Jing, D. Insights into the rheological behavior of ethanol-based metal oxide nanofluids. *J. Mol. Liq.* **2021**, *323*, 115006. [[CrossRef](#)]
45. Amir, Y.B.; Adnan, Q. Viscosity of CuO nanofluids: Experimental investigation and modelling with FFBP-ANN. *Thermochim. Acta* **2022**, *714*, 179267.
46. Kole, M.; Dey, T.K. Viscosity of alumina nanoparticles dispersed in car engine coolant. *Exp. Therm. Fluid Sci.* **2010**, *34*, 677–683. [[CrossRef](#)]

47. Chen, Y.; Huang, Y.; Li, K. Temperature effect on the aggregation kinetics of CeO<sub>2</sub> nanoparticles in monovalent and divalent electrolytes. *J. Environ. Anal. Toxicol.* **2012**, *2*, 158–162.
48. Maxwell, J. A physical treatise on electricity and magnetism. *J. Frankl. Inst.* **1881**, *111*, 386–389.
49. Einstein, A. Eine neue bestimmung der moleküldimensionen. *Ann. Phys.* **1906**, *324*, 289–306. [[CrossRef](#)]
50. Brinkman, H. The viscosity of concentrated suspensions and solutions. *J. Chem. Phys.* **1952**, *20*, 571. [[CrossRef](#)]
51. Batchelor, G.K. The effect of Brownian motion on the bulk stress in a suspension of spherical particles. *J. Fluid Mech.* **1977**, *83*, 97. [[CrossRef](#)]
52. Wang, X.; Xu, X.; Choi, S.U. Thermal conductivity of nanoparticle-fluid mixture. *J. Thermophys. Heat Transf.* **1999**, *13*, 474–480. [[CrossRef](#)]

**Disclaimer/Publisher’s Note:** The statements, opinions and data contained in all publications are solely those of the individual author(s) and contributor(s) and not of MDPI and/or the editor(s). MDPI and/or the editor(s) disclaim responsibility for any injury to people or property resulting from any ideas, methods, instructions or products referred to in the content.